Rapid Communications

Decreasing activation energy of fast relaxation processes in a metallic glass during aging

Martin Luckabauer, Tomoki Hayashi, Hidemi Kato, and Tetsu Ichitsubo
Institute for Materials Research, Tohoku University, Sendai 980-8577, Japan

(Received 4 December 2018; published 19 April 2019)

Many of the macroscopic properties of a glass are determined by the degree of structural relaxation. When the nonequilibrium system ages toward a thermodynamically more favorable state, the accompanying densification leads to an increase of the activation energies found for the α and especially the β relaxation processes. In this work we experimentally quantify the low-energy mechanical relaxation spectrum of a metallic glass at cryogenic temperatures, and show that these relaxation processes intriguingly show the opposite trend. The energy scale as well as the relaxation strength decrease during the aging process below the glass transition temperature with a surprisingly strong dependence on the annealing time. The experimental results are analyzed in the framework of established models and the temporal behavior of the typical energy V_0 is assessed. We compare the derived values to the values of the thermal energy available at the estimated fictive temperature of the given state and find that the absolute values as well as their temporal behavior show a high degree of correlation for the studied metallic glass. The decreasing characteristic energy values found in the present experiment directly depict the evolution of the structure toward a hypothetical lowest entropy state before the glass becomes structurally indistinguishable from a crystalline material.

DOI: 10.1103/PhysRevB.99.140202

In general, the physical properties of a glass depend significantly on the thermophysical history of the material, i.e., on the structural relaxation state. A detailed knowledge of this quantity is of great scientific and technological importance, because it determines important properties such as ductility, mechanical fatigue limit, or acoustic damping [1–5]. During structural relaxation the free volume in the glassy structure decreases and as a consequence the activation energies for diffusional processes tend to increase [6]. Since the fundamental defects probed in anelastic relaxation experiments on, e.g., the β relaxation are thought to be complex diffusional rearrangements [7], the activation energy for those processes also becomes larger during aging. Compared to crystalline materials, glasses show a variety of unique thermodynamic and vibrational features. At low temperatures an excess in the specific heat as well as a constant thermal conductivity is found [8–13]. These properties are usually associated with a low-frequency anomaly in the vibrational density of states, the so-called boson peak [14]. While it is ubiquitous in all glasses, the question whether or not the boson peak originates from structural peculiarities of the glass is still a highly debated topic [15–17]. In line with the thermal anomalies, also the acoustics of glasses at low temperatures are remarkably different from those of crystalline materials. Especially the low-temperature sound absorption was therefore the subject of numerous studies in the past and remains an actively investigated area [18–25]. Compared to crystalline materials the acoustic damping at low temperatures is found to be significantly stronger, a phenomenon usually explained in terms of interactions of the sound wave with two-level systems [26,27], causing internal friction. For the thermally activated regime Gilroy and Phillips developed a model based on asymmetric double-well potentials (ADWPs) [28]. The basic idea of this model is that the internal friction is caused by the anelastic relaxation of individual ADWPs which come into resonance with the acoustic wave. The energy and asymmetry distributions of those potentials are characteristic for the investigated glass and its configurational state. This concept in its original from as well as in some variations was successfully applied to describe the low-temperature damping behavior over a wide range of frequencies [4,29–31].

In contrast to previous studies, we choose a distinctly different approach. Instead of refining a model's capability to describe the low-temperature anomalies, we rather use established concepts to experimentally probe different structural relaxation states of a glass with the intention to link the characteristic parameters from theory to the properties of the material. As a model system we use the bulk metallic glass $Zr_{52.5}Ti_5Cu_{17.9}Ni_{14.6}Al_{10}$ (Vit105) mainly because of its good glass forming ability and the metallic character of all the constituents. Moreover, the glass transition temperature (T_g) for this material is known over a very large range of heating rates, which is especially important for the determination of a long-time sub-T_g annealing temperature for structural relaxation [32].

The experiments were performed in a self-developed electromagnetic acoustic resonance (EMAR) spectrometer, based on a Nb_3Sn superconducting magnet which allows for magnetic flux densities of up to 10 Tesla. In EMAR spectroscopy a mechanical vibration of defined frequency is created in the sample by the interaction of electromagnetically induced eddy currents with an external magnetic field [33–35]. The damping of the sample is assessed by measuring the time constant α of the free vibration decay which is detected by a receiver coil via the inverse Lorentz force mechanism. In terms of the decay constant the internal friction can be defined as $Q^{-1} = \alpha/(\pi f)$, where f is the frequency. The central advantage of the method is its noncontacting

principle, a property especially useful with very low damping materials.

To assure similarity of the as-cast condition all the samples for the measurements were cut from the same master rod. Cylinders of length 7.8 mm and diameter 3.85 mm were subjected to structural relaxation in evacuated glass ampules at 583 K, which is 80 K below the calorimetrically determined glass transition at 5 K/min heating rate.

Assuming anelastic relaxation of a distribution of thermally activated ADWPs with energy V and intrinsic asymmetry Δ, the internal friction of a bulk sample can be expressed as [28,31]

$$Q^{-1} = \frac{\gamma^2}{\rho v^2 k_B T} \int_{-\infty}^{\infty} d\Delta \int_0^{\infty} dV P(\Delta, V) \times \operatorname{sech}^2\left(\frac{\Delta}{2k_B T}\right) \frac{\omega\tau}{1+\omega^2\tau^2}. \quad (1)$$

In this relation, ρ is the mass density, v is the speed of sound, k_B is the Boltzmann constant, and T is the absolute temperature. The important quantity $\gamma = 1/2\ d\Delta/d\epsilon$ is the deformation potential which describes the sensitivity of the asymmetry Δ on the strain ϵ caused by the sound wave and is therefore responsible for the relaxation strength. As usual the speed of sound v depends on the polarization of the wave and consequently on the experimental conditions. In order to be able to capture experimental data it is crucial to find a distribution function $P(\Delta, V)$ capable of depicting the physical situation. To keep this work comparable to almost all preceding experimental studies [4,28,29,31] on two-level systems we use the factorization $P(\Delta, V) = f(\Delta)g(V)$, but not without mentioning its inconsistencies. Most generally V and Δ cannot be statistically independent since the asymmetry Δ must at least satisfy the condition $\Delta < 2V$ because otherwise unphysical systems with no barrier emerge. Moreover, it is well known from theoretical works on silica that the coupled distribution $P(\Delta, V)$ is very different from the separable one, especially if a large range of asymmetries and barrier heights is considered. A satisfying agreement is only found if both Δ and V are sufficiently small which in the case of silica also corresponds to the range where both the coupled and the uncoupled distributions have the highest densities [36]. This also implies that measurements on glasses where small barriers and asymmetries are dominant can be sufficiently well described by an uncoupled distribution. Based on the experimental results obtained in this study and for the sake of comparability we assume that for the glass used and the chosen measurement conditions the factorization can be justified. We follow an idea by Vacher [31], who assumed a distribution function for the characteristic potentials $g(V)$ inspired by the soft potential model (SPM) [37–39],

$$g(V) \propto \left(\frac{V}{V_0}\right)^{-\zeta} \exp\left(-\frac{1}{2}\frac{V^2}{V_0^2}\right). \quad (2)$$

From the SPM the exponent ζ is predicted to be $1/4$, a value experimentally confirmed for silica [29,31] but not for other glass formers [29]. Since, a conclusive link to structural properties cannot be established, we assume ζ to be of characteristic value for the glass under consideration. The quantity V_0 determines the energy scale of the distribution and is

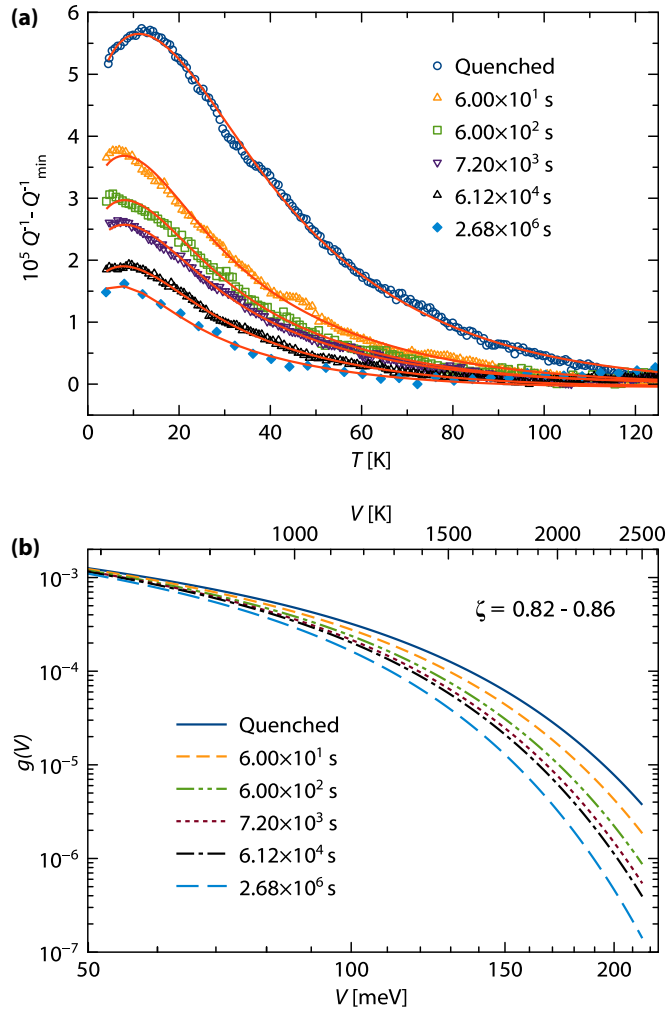

FIG. 1. (a) Cryogenic internal friction measurements for different structural relaxation states. In all cases the annealing temperature is 583 K, which is 80 K below the calorimetrically determined glass transition temperature for the unrelaxed sample. The solid lines represent the best fits to the data according to Eq. (1). For a better comparison the minimum friction value is subtracted from all data sets. Each data point was measured in acoustic resonance of the same resonance mode at around 700 kHz. The resonance frequency change as a function of temperature is shown in Fig. S1 of the Supplemental Material [40]. Panel (b) shows the distribution functions $g(V)$ according to Eq. (2) for the determined V_0 and ζ values.

therefore intimately linked to the microscopic configuration of the glass. The dependence of this parameter on the structural relaxation state is the central question upon which this work is based. For the asymmetry distribution we use a Gaussian with characteristic cutoff energy Δ_C,

$$f(\Delta) \propto \exp\left(-\frac{1}{2}\frac{\Delta^2}{\Delta_C^2}\right). \quad (3)$$

Like in previous studies this choice is motivated by the assumption that neither positive nor negative asymmetries are preferred.

The experimental results for the internal friction Q^{-1} are shown in Fig. 1(a). Compared to crystalline materials the

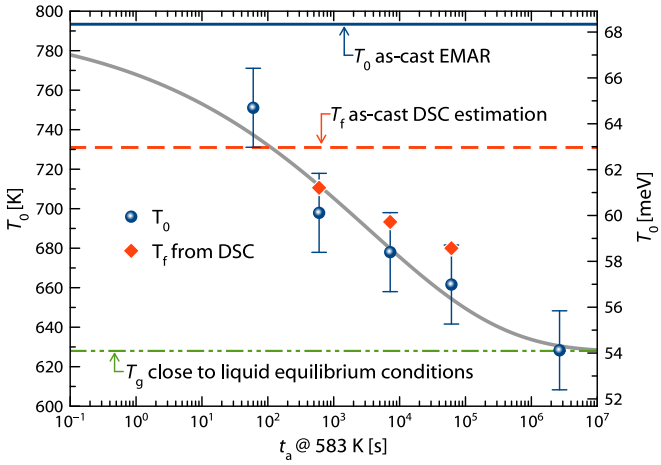

FIG. 2. The evolution of the characteristic temperature $T_0 = V_0/k_B$ with annealing time. The values derived from the best fits of Eq. (1) to the data (blue circles) are compared to values for the fictive temperature T_f (red diamonds) obtained by DSC measurements at 10 K/min. The values obtained for the as-quenched condition are shown by the solid blue line (T_0 value from internal friction) and the dashed red line (T_f from DSC). The bottom line represents the lowest measured glass transition temperature, close to liquid equilibrium conditions [32] and is given for comparison. A stretched exponential function is used to capture the temporal behavior.

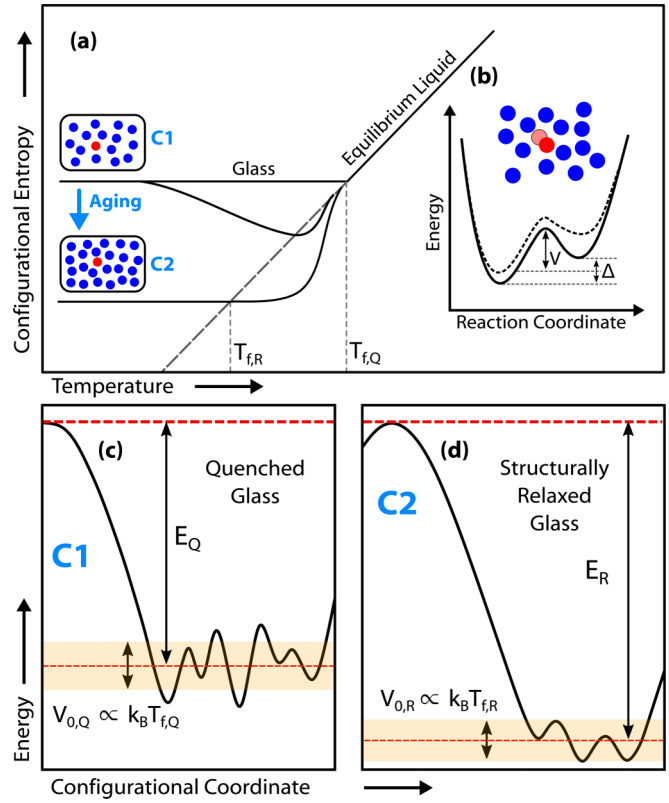

FIG. 3. The origin of the two-level systems and the impact of structural relaxation. In (a) the change of configurational entropy of a glass with temperature and time is shown. After rapid cooling an open structure (C1) with a high fictive temperature $T_{f,Q}$ is obtained. Upon structural relaxation the glass densifies and the structure is described by a new fictive temperature $T_{f,R}$. In both cases the measurement of T_g by DSC (curved traces) gives approximately the same result. In the inset (b) an unstressed (solid line) and a stressed (dashed line) asymmetric double-well potential (ADWP), corresponding to two atomic configurations is shown. An external perturbation can bring the ADWP out of equilibrium (dashed line) which then returns back with a characteristic relaxation time. If a periodic perturbation matches the inverse of the relaxation time, resonance is observed. In condition C1 (c) the ADWP landscape is rough and comprises larger energy amplitudes than in the structurally relaxed glass C2 (d). The energy necessary for particle rearrangement (E_Q and E_R) increases during structural relaxation, while the characteristic energy of the ADWPs, V_0, decreases.

damping of the acoustic wave does not show a freeze-out effect (i.e., a constant low value at very low temperatures), but rather starts to increase at around 110 K, culminating in a maximum at a temperature of a few kelvin. To better compare the results, the minimum value $Q^{-1}_{\min}$ of the damping is subtracted from each dataset. The difference in the data for the different structural relaxation states is obvious, showing a strong decrease even after only 60 s of annealing. This is a surprising finding, since the structural rearrangements at the annealing temperature of 583 K ($\approx$87% of the glass transition temperature at 5 K/min) are expected to be very slow. On the other hand, it suggests that minor structural reconfigurations can have a significant impact on the properties of the glass. The results for all conditions are very well captured by the model defined by Eqs. (1) and (2). In Fig. 1(b) the distribution functions $g(V)$ are shown. To better assess the spreading of the functions at higher energies, the minimum abscissa value was set to 50 meV. A detailed overview of all the parameters can be found in Supplemental Table S1 [40].

From the fits to the data the value of the characteristic energy $V_0 = k_B T_0$ from Eq. (2) was extracted and is plotted in Fig. 2 as a function of structural relaxation time. The value for the as-quenched condition is shown as a horizontal base line in the logarithmic plot. During relaxation the value gradually decreases toward 628 K after 31 days of annealing. Structural relaxation (enthalpy or volume) of metallic glasses as a function of time is usually described by a stretched exponential function of the form $X(t) = X_a[1 - \exp[(-t/\tau^*)^\beta]]$, where X is either volume or enthalpy. Hence, if V_0 is a characteristic parameter of the relaxation state it should also follow this functional form. The fit to the derived values is shown in Fig. 2 and within the uncertainty limits they are well described by a stretched exponential with parameters $\tau^* = (3442 \pm 1000)$ s and $\beta = (0.21 \pm 0.08)$, corresponding to a mean structural relaxation time $\langle\tau\rangle = 2.77 \times 10^5$ s at 583 K ($\langle\tau\rangle = (\tau^*/\beta) \times \Gamma(1/\beta)$, where Γ is the gamma function). For comparison we also show the values for the fictive temperature T_f derived from differential scanning calorimetry (DSC) measurements. An intriguing correlation between the values for T_0 and T_f is found, indicating an intimate link between the two parameters. The DSC measurements are shown in Supplemental Material Fig. S2 together with the mathematical description of the fictive temperature determination [40].

We now turn to the possible origins of the link between the structural relaxation state (or fictive temperature) and the characteristic parameter of the potential energy distribution. In Fig. 3(a), the cooling process for a glass (at one exemplary

linear cooling rate) in terms of its configurational entropy, is shown schematically. At high temperatures the structural reconfigurations, necessary to establish thermal equilibrium, can follow the temperature change, since the timescale of diffusion is much smaller than the timescale of cooling. At a certain point in the process this relation reverses rather fast and the diffusional degrees of freedom quickly get frozen with respect to the timescale of cooling—the liquid transforms into a glass. Accordingly, the configuration [C1 in Fig. 3(a)] resembles the configuration of the liquid at $T_{f,Q}$. This inherent glass transition temperature is called the fictive temperature because it is not directly accessible in experiments, yet it determines the properties of the glass. Upon aging, i.e., annealing at temperatures below $T_{f,Q}$ but sufficiently high for diffusional reconfigurations, the configurational entropy of the glass slowly decreases and the newly formed structure in principle corresponds to a new T_f, $T_{f,R}$ in Fig. 3(a). The link between the potential energy distribution in the completely frozen glass structure and T_f most likely arises from a correspondence of the mean volume available for each particle in the liquid and the energy necessary for particle displacement in the glass. In the equilibrium liquid the specific volume is time independent and it changes with a thermal expansion coefficient specific for the system under consideration. In the case of Vit105 this coefficient is 5.65×10^{-5} K^{-1} at around the equilibrium melting temperature [41]. When the liquid falls out of equilibrium at a fictive temperature, the volume of the liquid is conserved in the glass and can serve as space for particle oscillations at low temperatures. In Fig. 3(b) two nearly equivalent atomic positions in the glass exemplary correspond to the depicted double-well potential. A minor change in the specific volume of the structure, either by a different cooling rate from the liquid or by aging below the glass transition, changes also the double-well potentials in terms of their energy. It is important to note that the characteristic value $T_0 = V_0/k_B$ determines the energy scale of a distribution, reflecting the specific distribution of free volume in the structure. Upon aging, systems with a large energy amplitude, corresponding to a large local excess volume, preferably anneal out because of a high local driving force. Overall the ground-state energy of the two-level systems has to decrease in order to minimize the free energy of the glass. The situation is shown in Figs. 3(c) and 3(d) for the two structural configurations C1 and C2. The energies E_Q and E_R are the energies necessary for particle rearrangement (order of electron volts in metallic glasses) and increase during the densification process upon structural relaxation. At the same time as a consequence of the densification and the increase in short-range order, the "roughness" of the double-well potentials decrease and so does the parameter V_0. In this picture a hypothetical ideal glass state would correspond to the lowest possible interbasin roughness just before the glassy structure becomes indistinguishable to a crystal with only one stable atomic configuration.

The numerical equivalency of T_0 and the fictive temperature T_f is an unexpected finding. On one hand it can be assumed that the spontaneous overcoming of the double-well potentials is a prerequisite for the glass transition, but on the other hand, this does not conclusively explain the equivalency found in this study. While for network glasses, especially SiO_2, the values for V_0 are only between 20% and 50% of the glass transition temperature [4,29,31], the value found for amorphous selenium (a-Se) is again very close to the glass transition temperature and could well reflect the fictive temperature of the material [29]. The metallic glass used here and a-Se share one important property: in both glasses the structural units are atoms. In SiO_2 the structural units are interlinked SiO_4 tetrahedra, thus representing molecules. We assume that in an internal friction experiment either intramolecular degrees of freedom are probed (e.g., rattling of Si within the tetrahedra) which are not directly linked to the glass transition temperature or the coupling of the higher energy systems to the elastic wave is significantly worse. The latter assumption is also supported by recent computer simulations [25]. Another important point is the general validity of the distribution function Eq. (2). There is strong evidence that at least certain metallic glasses exhibit static heterogeneity in their structure [42,43]. In such a case it can be expected that the description of the distribution by a smooth function is only approximately possible and that a direct numerical treatment of Eq. (1) is the more appropriate way to obtain structural information.

Structural relaxation or rejuvenation (which is the opposite) are the processes controlling the properties of a glass. The concept of fictive temperature for their characterization is in principle an elegant way for predicting properties [5,44]. However, since there is no direct access to the value the determination relies on the validity of the extrapolation of thermodynamic measurements. Especially for strongly relaxed or highly rejuvenated glasses this implies large uncertainties or even impedes any statement. In comparison, low-temperature internal friction measurements possess none of these drawbacks: it is an absolute technique which requires no reference state, a measurement on the same sample can be repeated, the degree of relaxation/rejuvenation has no influence on the uncertainties, and additional structural information about the glass can be obtained.

Most importantly, the present measurements show that the anelastic relaxation spectrum of glasses contains both—processes with increasing and decreasing activation energy during aging. Processes like the slow β relaxation where resonance of the driving oscillation with diffusional defects occurs, show an increase in activation energy since the densification renders atomic rearrangements more difficult. On the other hand, the low-energy transitions probed here have to decrease in energy since the atomic positions become more and more stable and the potential energy landscape between two metastable atomic configurations becomes smoother and more defined. Finally, it should be noted that in contrast to high-temperature phenomena like the β relaxation where aging is inevitable during any experiment, the low-temperature relaxations probed in this work are fully reversible and stable in time. Consequently, we expect that the present results can be more easily confirmed by computer simulations than results from classical relaxation experiments.

M.L. would like to thank D. Rodney for the valuable discussion about the physical fundamentals of two-level systems in glasses.

[1] J. J. Kruzic, Adv. Eng. Mater. **18**, 1308 (2016).
[2] W. Wang, C. Dong, and C. Shek, Mater. Sci. Eng., R **44**, 45 (2004).
[3] T. Egami, T. Iwashita, and W. Dmowski, Metals **3**, 77 (2013).
[4] F. Travasso, P. Amico, L. Bosi, F. Cottone, A. Dari, L. Gammaitoni, H. Vocca, and F. Marchesoni, Europhys. Lett. **80**, 50008 (2007).
[5] G. Kumar, P. Neibecker, Y. Liu, and J. Schroers, Nat. Commun. **4**, 1536 (2013).
[6] F. Faupel, W. Frank, M.-P. Macht, H. Mehrer, V. Naundorf, K. Rätzke, H. R. Schober, S. K. Sharma, and H. Teichler, Rev. Mod. Phys. **75**, 237 (2003).
[7] H.-B. Yu, R. Richert, and K. Samwer, Sci. Adv. **3**, e1701577 (2017).
[8] A. Antoniou and J. Morrison, J. Appl. Phys. **36**, 1873 (1965).
[9] P. Anderson, B. Halperin, and C. Varma, Philos. Mag. **25**, 1 (1972).
[10] M. P. Zaitlin and A. C. Anderson, Phys. Status Solidi B **71**, 323 (1975).
[11] Y. Li, P. Yu, and H. Y. Bai, Appl. Phys. Lett. **86**, 231909 (2005).
[12] Y. Li, H. Y. Bai, W. H. Wang, and K. Samwer, Phys. Rev. B **74**, 052201 (2006).
[13] B. Huang, H. Y. Bai, and W. H. Wang, J. Appl. Phys. **115**, 153505 (2014).
[14] W. Schirmacher, Phys. Status Solidi B **250**, 937 (2013).
[15] A. I. Chumakov, G. Monaco, A. Monaco, W. A. Crichton, A. Bosak, R. Rüffer, A. Meyer, F. Kargl, L. Comez, D. Fioretto, H. Giefers, S. Roitsch, G. Wortmann, M. H. Manghnani, A. Hushur, Q. Williams, J. Balogh, K. Parliński, P. Jochym, and P. Piekarz, Phys. Rev. Lett. **106**, 225501 (2011).
[16] D. Crespo, P. Bruna, A. Valles, and E. Pineda, Phys. Rev. B **94**, 144205 (2016).
[17] T. Brink, L. Koch, and K. Albe, Phys. Rev. B **94**, 224203 (2016).
[18] R. Strakna and H. Savage, J. Appl. Phys. **35**, 1445 (1964).
[19] J. Jäckle, Z. Phys. A **257**, 212 (1972).
[20] S. Hunklinger, W. Arnold, and S. Stein, Phys. Lett. A **45**, 311 (1973).
[21] M. Barmatz and H. S. Chen, Phys. Rev. B **9**, 4073 (1974).
[22] J. Bonnet, J. Non-Cryst. Solids **127**, 227 (1991).
[23] S. Rau, C. Enss, S. Hunklinger, P. Neu, and A. Würger, Phys. Rev. B **52**, 7179 (1995).
[24] T. Damart, A. Tanguy, and D. Rodney, Phys. Rev. B **95**, 054203 (2017).
[25] T. Damart and D. Rodney, Phys. Rev. B **97**, 014201 (2018).
[26] S. Hunklinger and W. Arnold, in *Physical Acoustics*, edited by W. P. Mason and R. Thurston (Academic, New York, 1976), Vol. 12, pp. 155–215.
[27] W. A. Phillips, Rep. Prog. Phys. **50**, 1657 (1987).
[28] K. S. Gilroy and W. A. Phillips, Philos. Mag. B **43**, 735 (1981).
[29] R. Keil, G. Kasper, and S. Hunklinger, J. Non-Cryst. Solids **164-166**, 1183 (1993).
[30] E. Rat, M. Foret, G. Massiera, R. Vialla, M. Arai, R. Vacher, and E. Courtens, Phys. Rev. B **72**, 214204 (2005).
[31] R. Vacher, E. Courtens, and M. Foret, Phys. Rev. B **72**, 214205 (2005).
[32] M. Luckabauer, U. Kühn, J. Eckert, and W. Sprengel, Phys. Rev. B **89**, 174113 (2014).
[33] M. Hirao and H. Ogi, *Electromagnetic Acoustic Transducers: Noncontacting Ultrasonic Measurements using EMATs*, Springer Series in Measurement Science and Technology (Springer Japan, 2016).
[34] H. Ogi, M. Hirao, T. Honda, and H. Fukuoka, Rev. Prog. Quant. Nondestr. Eval. **14**, 1601 (1995).
[35] H. Ogi, H. Ledbetter, S. Kim, and M. Hirao, J. Acoust. Soc. Am. **106**, 660 (1999).
[36] C. R. Billman, J. P. Trinastic, D. J. Davis, R. Hamdan, and H.-P. Cheng, Phys. Rev. B **95**, 014109 (2017).
[37] V. G. Karpov, M. I. Klinger, and F. N. Ignat'ev, Sov. Phys. JETP **57**, 439 (1983).
[38] Y. M. Galperin, V. L. Gurevich, and D. A. Parshin, Phys. Rev. B **32**, 6873 (1985).
[39] U. Buchenau, Y. M. Galperin, V. L. Gurevich, D. A. Parshin, M. A. Ramos, and H. R. Schober, Phys. Rev. B **46**, 2798 (1992).
[40] See Supplemental Material at http://link.aps.org/supplemental/10.1103/PhysRevB.99.140202 for details about the sample preparation, acoustic resonance measurements, calculation of the fictive temperature, and x-ray diffraction results.
[41] A. K. Gangopadhyay, C. E. Pueblo, R. Dai, M. L. Johnson, R. Ashcraft, D. Van Hoesen, M. Sellers, and K. F. Kelton, J. Chem. Phys. **146**, 154506 (2017).
[42] T. Ichitsubo, E. Matsubara, T. Yamamoto, H. S. Chen, N. Nishiyama, J. Saida, and K. Anazawa, Phys. Rev. Lett. **95**, 245501 (2005).
[43] S. Ketov, Y. Sun, S. Nachum, Z. Lu, A. Checchi, A. Beraldin, H. Bai, W. Wang, D. Louzguine-Luzgin, M. Carpenter, and A. Greer, Nature (London) **524**, 200 (2015).
[44] J. Ketkaew, W. Chen, H. Wang, A. Datye, M. Fan, G. Pereira, U. Schwarz, Z. Liu, R. Yamada, W. Dmowski, M. Shattuck, C. O'Hern, T. Egami, E. Bouchbinder, and J. Schroers, Nat. Commun. **9**, 3271 (2018).